Cross sections and ion kinetic energy analysis for the electron impact ionization of acetylene

S. Feil, K. Głuch,[a] A. Bacher, S. Matt-Leubner, D. K. Böhme,[b] P. Scheier, and T. D. Märk[c]
Institut für Ionenphysik, Leopold-Franzens Universität Innsbruck, Technikerstrasse 25, A-6020 Innsbruck, Austria

(Received 27 February 2006; accepted 12 April 2006; published online 6 June 2006)

Using a Nier-type electron impact ion source in combination with a double focusing two sector field mass spectrometer, partial cross sections for electron impact ionization of acetylene are measured for electron energies up to 1000 eV. Discrimination factors for ions are determined using the deflection field method in combination with a three-dimensional ion trajectory simulation of ions produced in the ion source. Analysis of the ion yield curves obtained by scanning the deflectors allows the assignment of ions with the same mass-to-charge ratio to specific production channels on the basis of their different kinetic energy distributions. This analysis also allows to determine, besides kinetic energy distributions of fragment ions, partial cross sections differential in kinetic energy. Moreover a charge separation reaction, the Coulomb explosion of the doubly charged parent ions $C_2H_2^{++}$ into the fragment ions C_2H^+ and H^+, is investigated and its mean kinetic energy release ($\langle KER \rangle = 3.88$ eV) is deduced. © *2006 American Institute of Physics*. [DOI: 10.1063/1.2202317]

I. INTRODUCTION

Acetylene is an important molecule in various fields such as the semiconductor industry,[1] edge plasmas in fusion reactors[2] and interstellar plasmas.[3,4] Its interaction with electrons, photons, and ions has been studied intensively. However, not many investigations have been devoted to the measurement of absolute total and partial electron impact ionization cross sections, despite the fact that these data are needed for modeling C_2H_2-containing plasmas. Furthermore, modelers need to know not only the production efficiency for a specific ion but also its kinetic energy distribution, because the large number of ensuing ion-molecule reactions in the plasma, the confinement times, and the plasma-wall interactions depend on this energy. A given fragment ion may be produced via different dissociation processes that release different amounts of kinetic energy. For instance C_2H^+ can be formed via neutral H loss from an excited $C_2H_2^{+*}$ or via Coulomb explosion of $C_2H_2^{++}$ into $C_2H^+ + H^+$. Doubly charged ions are produced at higher electron energies and the fragment cations that are formed via the Coulomb decay process have typically higher kinetic energies than the same fragment ions that are formed via dissociation of a singly charged precursor ion. Knowledge of these facts is of fundamental importance for energy balancing of plasma sheaths that are formed in fusion devices.

The first ionization cross section experiment of acetylene was performed in 1932 by Tate and Smith[5] who measured the total ion production efficiency for the interaction with electrons in the energy range of 15–500 eV. A few years later they also measured relative partial ionization efficiency curves and combined the results of these two experiments to obtain the absolute total and partial ionization cross sections.[6] In 1967 Gaudin and Hagemann[7] determined partial electron impact ionization cross sections for acetylene for energies between 100 and 2000 eV. Also Zheng and Srivastava[8] measured electron impact cross sections for the formation of the parent and fragment ions from the threshold to 800 eV.

However, none of these earlier experiments was specifically designed to measure energetic fragment ions, and thus they could not take into account the dependence of the collection efficiency on the kinetic energy of the ions produced. Ions with a high kinetic energy are more discriminated against a mass spectrometer than ions with a low kinetic energy. Thus the cross sections obtained for ions produced with higher kinetic energies, i.e., up to a few eV, are generally considered to be too low.[9] In the recent review of Shirai *et al.*[10] the total ionization cross section for acetylene determined by Tian and Vidal[11] is recommended because these latter authors demonstrated a complete collection of all ions, including the energetic ones. Tian and Vidal did not measure directly the total ionization cross section, but summed up all partial cross sections to obtain the total cross section. As expected, the data for light fragments (which usually carry more kinetic energy[9] of Tian and Vidal) are higher than the values published previously.[5–8]

As mentioned above, for the purpose of modeling plasma chemistry and plasma dynamics, both the correct absolute cross sections and the energy distributions of the produced ions are required. Despite this urgent need for data, only a few studies have measured cross sections that are differential with respect to the kinetic energy of the ions. Davister and Locht examined in detail the dissociative ionization of acetylene[12–14] for electron energies up to 99 eV.

[a]Permanent address: Department of Physics, University Marie Curie Sklodowskiej, Lublin, Poland.
[b]Also at Department of Chemistry, York University, 4700 Keele Street, Toronto, M3J 1P3, Canada.
[c]Author to whom correspondence should be addressed. Electronic mail: Tilmann.Maerk@uibk.ac.at

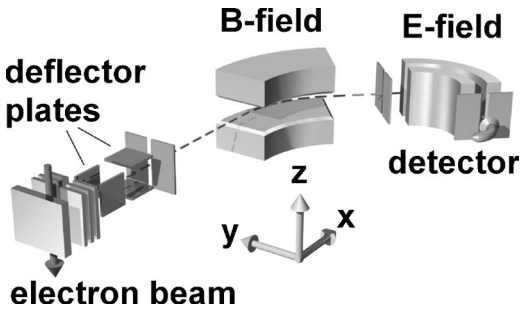

FIG. 1. Schematic view of the experimental setup.

Their studies were focused on the accurate determination of appearance energies and translational energies of the various fragment ions produced by electron impact, but not on the determination of accurate cross sections. Using the onset energies and the corresponding translational energies of the ions, they could attribute the production of these ions to specific reaction channels. They investigated in detail the production of H^+ and C_2H^+,[11] CH^+,[12] and CH^+, C^+, and CH_2^+.[13] Similar measurements are described in the present paper. However, our main goal here is to determine partial cross sections that are differential with respect to the kinetic energies for fragment ions up to electron energies of 1000 eV, and not to determine accurate appearance energies which already have been reported earlier (e.g., Refs. 15–19).

II. EXPERIMENT

All measurements are taken with a double focusing two sector field mass spectrometer of reversed geometry combined with a modified Nier-type electron-impact ion source (see Fig. 1). A detailed description of this setup is given elsewhere.[20–22] The neutral gas is introduced through a capillary leak gas inlet and crossed by an electron beam of variable energy, i.e., from about 0 to 1000 eV, with an energy spread of approximately 0.5 eV full width at half maximum (FWHM). The electron current is kept low for cross section measurements, i.e., about 10 μA, to assure single collision conditions during the ionization process. The ions produced are immediately extracted from the center of the ion source by a weak penetrating electric field. However, ions with a high initial kinetic energy, e.g., fragment ions that are produced in the ion source via Coulomb explosion of doubly charged precursor ions, may hit the walls in the ion source and will be lost. In order to take this factor into account we can apply stronger extraction fields (3 kV/m) which allow for the collection of ions with a kinetic energy up to 10 eV. These conditions have been used for monitoring ion beam profiles (so called z profiles).

After extracting the ions out of the ion source, they are accelerated to $q \times 3$ kV, where q is the charge state of the corresponding ion. Between the collision chamber and the entrance slit of the mass spectrometer the ions pass two pairs of perpendicular deflection plates which allow steering of the ion beam to obtain maximum ion yield at the detector. However, for cross section measurements, these deflection plates are used to sweep the extracted ion beam across the entrance slit[22,23] in the y and z directions (see Fig. 1). The ion signal is

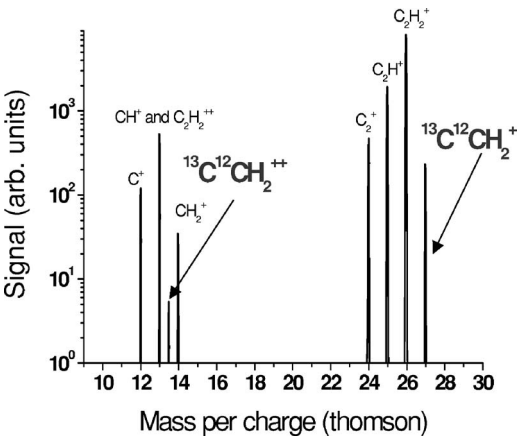

FIG. 2. Mass spectrum of acetylene recorded at an electron energy of 100 eV and an electron current of 370 μA corrected for background contributions and for discrimination effects (see text).

then recorded as a function of the applied voltage and is integrated to obtain the total ion yield for a specific electron energy. After passing the entrance slit, the ions pass a first field-free region, then pass a magnetic sector field which selects ions according to their momentum, followed by an electric sector field which selects ions according to their kinetic energy. Finally, the ions are detected by a channeltron-type electron multiplier operated in a counting mode. The combined action of the two sector fields in a double focusing mass spectrometer results in a focusing of the ions within the plane of the instrument accounting for angular and spatial spreads of the starting points of the ions and for small variations in their kinetic energy. However, there is no focusing effect in the direction perpendicular to this plane, i.e., the z direction. Thus only the z deflectors (Fig. 1) are used to compensate a velocity component outside of the plane of the instrument.

The initial velocity of an ion is a sum of the velocity of the neutral precursor molecule and the velocity that is released during the ionization event. The initial kinetic energy distribution of an ion is reflected in the z profile and can be determined by a special evaluation procedure described in detail in Ref. 24. A parent ion shows a narrow peak with a width that is determined by the thermal velocity distribution of the neutral precursor and the geometry of the ion source. Fragment ions, however, may have wider and more complex z profiles, especially if they are formed via different reaction pathways. If dissociation occurs after the precursor ion is fully accelerated, i.e., unimolecular metastable dissociation, the kinetic energy release (KER) can be determined via special scan techniques developed for sector field mass spectrometers.[25] One of these techniques allows a determination of the average KER with the mass analyzed ion kinetic energy (MIKE) scan as discussed in detail in Ref. 26.

III. RESULTS AND DISCUSSION

A mass spectrum of acetylene ionized by 100 eV electrons is shown in Fig. 2. The pressure is set to 1×10^{-4} Pa and the electron current is 370 μA. This mass spectrum is

corrected for the residual background and the discrimination effects due to the initial kinetic energies of the ions (see below).

Also shown in Fig. 2 are the isotopomers $^{13}C^{12}CH_2^+$ and $^{13}C^{12}CH_2^{++}$ which have an abundance of about 2% of the main isotopes $^{12}C_2H_2^+$ and $^{12}C_2H_2^{++}$, respectively. Since the $^{13}C^{12}CH_2^{++}$ ions appear at the noninteger mass-to-charge ratio of 13.5 thomson, this peak can be assigned unambiguously to the doubly charged acetylene ion, whereas the peak at mass of 13 consists of both $^{12}C_2H_2^{++}$ and $^{12}CH^+$ ions. The signal at 13.5 thomson is about 1.7% of the signal at 13 thomson. We therefore conclude that a major part of the signal at the mass to charge ratio of 13 can be assigned to the doubly charged parent ion and that the rest of the signal is due to the singly charged fragment ion CH^+. However, the contribution of the doubly charged ion clearly will depend strongly on the electron energy used for the ionization. In agreement with observations of Davister and Locht[12] and Thissen *et al.*[27] we observe that for electron energies lower than about 36 eV most of the ions at mass to charge ratio of 13 thomson have large kinetic energies ranging up to 4 eV (see below). The z profiles of the mass to charge ratio of 13 thomson in the upper diagram of Fig. 3 exhibit a strong increase of the low kinetic energy contribution at electron energies above 36 eV. Therefore, these ions with thermal kinetic energies are attributed to dications because no kinetic energy release is involved in the ionization process for these parent ions.

In order to elucidate this behavior of the z profiles, we analyzed these beam profiles in a more quantitative way (for details see Ref. 24). The initial ion kinetic energy distribution and the extraction efficiency (discrimination factor) from the ion source for a given product ion are determined by fitting measured ion beam z profiles with a superposition of simulated ion beam profiles. 2×10^6 ion trajectories are calculated at 57 different discrete initial kinetic energies of the respective product ion. The position where these ions are formed is randomly taken within the volume that is covered by the electron beam. Thereby, ion loss to the walls of the ion source housing is included in the resulting z profiles of the ion beam. Note that in the earlier method described by Poll *et al.*[20] the measured z profiles are assumed to be unaffected by reduced extraction efficiency. In contrast the present method of fitting a weighted superposition of three-dimensional (3D) simulated z profiles to the experimental data allows the analysis of ion beam profiles of highly energetic fragment ions that are affected by the reduced ion extraction efficiency.

As an example the ion beam profiles in the z direction for the fragment ions with m/z ratios of 13 and 14 (CH^+ and CH_2^+) measured at different electron energies are shown in Figs. 3 and 4 (upper panels). The output of the fitting procedure is a kinetic energy distribution and a corresponding discrimination factor for each fragment ion at each electron energy considered. The discrimination factors are a measure for the loss (due to their kinetic energy) during the extraction procedure of the ions produced in the ion source. Examples for ion kinetic energy distributions derived from z profiles are shown in the lower panels of Figs. 3 and 4. The kinetic

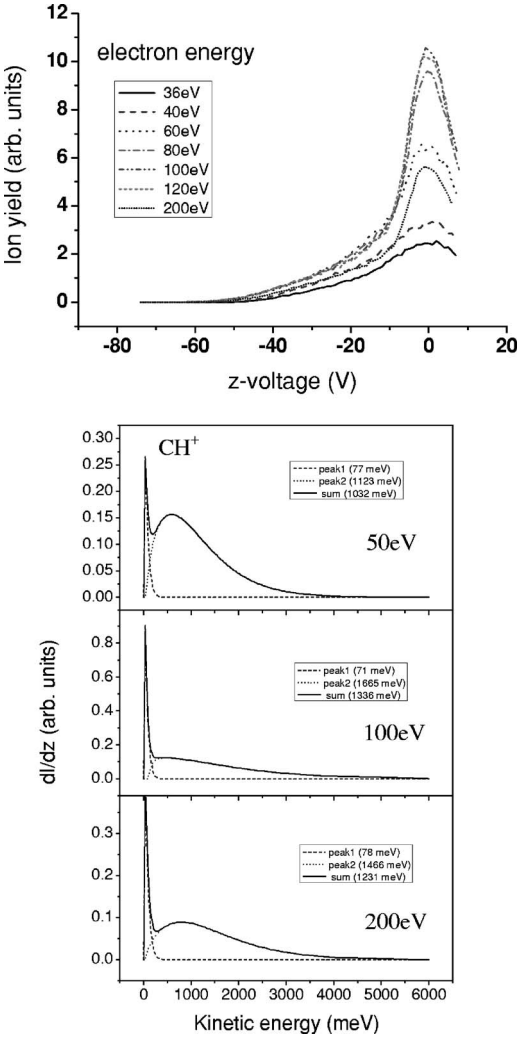

FIG. 3. Ion yield profiles (z profiles) of the CH^+ ion in the upper panel. Please note that from an electron energy of 40 eV onwards, only the thermal part of the signal is growing and the higher energy part is remaining at the same level. The lower panel represents kinetic energy distribution functions evaluated at different electron energies. Note that there are two contributions (low and high kinetic energy) to the resulting curve.

energy distributions obtained for the fragments with m/z ratios of 13 and 14 reveal a pronounced dependence on the electron energy.

As mentioned above the fitting procedures also provide a discrimination factor (=1/extraction efficiency) for each ion that depends on the kinetic energy of the fragment. Multiplication of the measured apparent partial cross sections with the corresponding discrimination factors provides a compensation for the reduced extraction efficiency, thus yielding accurate partial cross sections with the present experimental setup (see also Ref. 23 where this has been checked using previous data for CH_4). Although the kinetic energy distribution functions can differ slightly depending on the starting parameters in the calculations, the results for the discrimination factors are independent of these variations. Depending on the kinetic energy of the fragment ion (which depends on the incident electron energy), the values of the discrimination factors lie between 1.058 for the parent ion (which does not show any dependence on incident electron energy) and 2.12 for the C_2H^+ ion at 200 eV incident electron energy (see

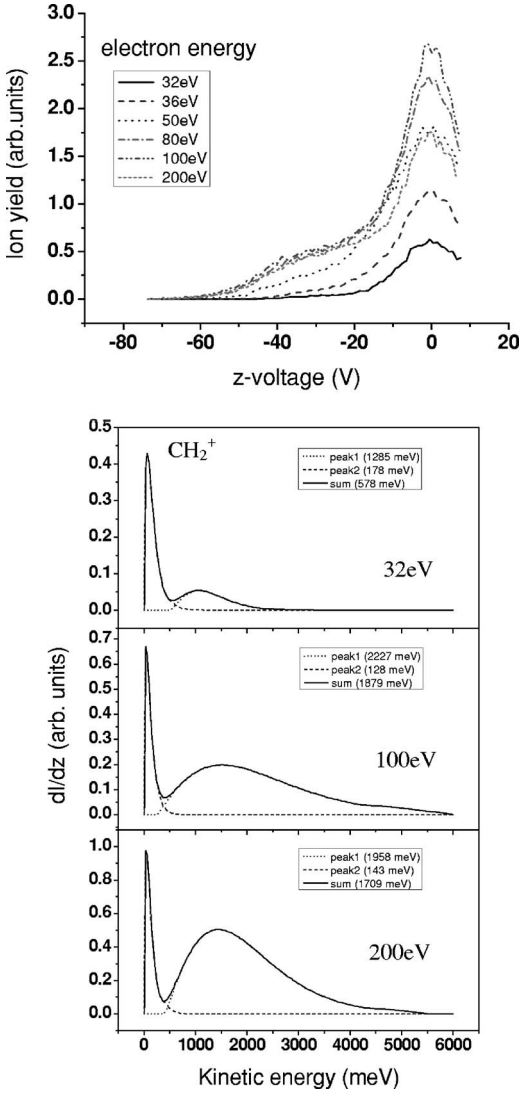

FIG. 4. Ion yield profiles (z profiles) of the CH_2^+ ion. The lower panel represents kinetic energy distribution functions evaluated at different electron energies.

Table I). The precision of the calculations is ±0.05 which corresponds to a maximum uncertainty of 10%.

The corrected absolute partial cross sections for the ions $C_2H_2^+$, C_2H^+, C_2^+, C^+, CH_2^+, and CH^+ are summarized in Fig. 5. Absolute cross sections are obtained by normalizing the sum of these partial cross sections at each electron energy with the corresponding absolute total cross sections obtained

TABLE I. Discrimination factors (see text) for various fragment ions at three different incident electron energies.

	Discrimination factor at		
Fragment ion	50 eV	100 eV	200 eV
C^+	1.96	1.96	2.05
CH^+	1.99	1.76	1.87
CH_2^+	1.98	1.98	2.12
C_2^+	1.13	1.12	1.12
C_2H^+	1.10	1.10	1.10
$C_2H_2^+$	1.06	1.06	1.06

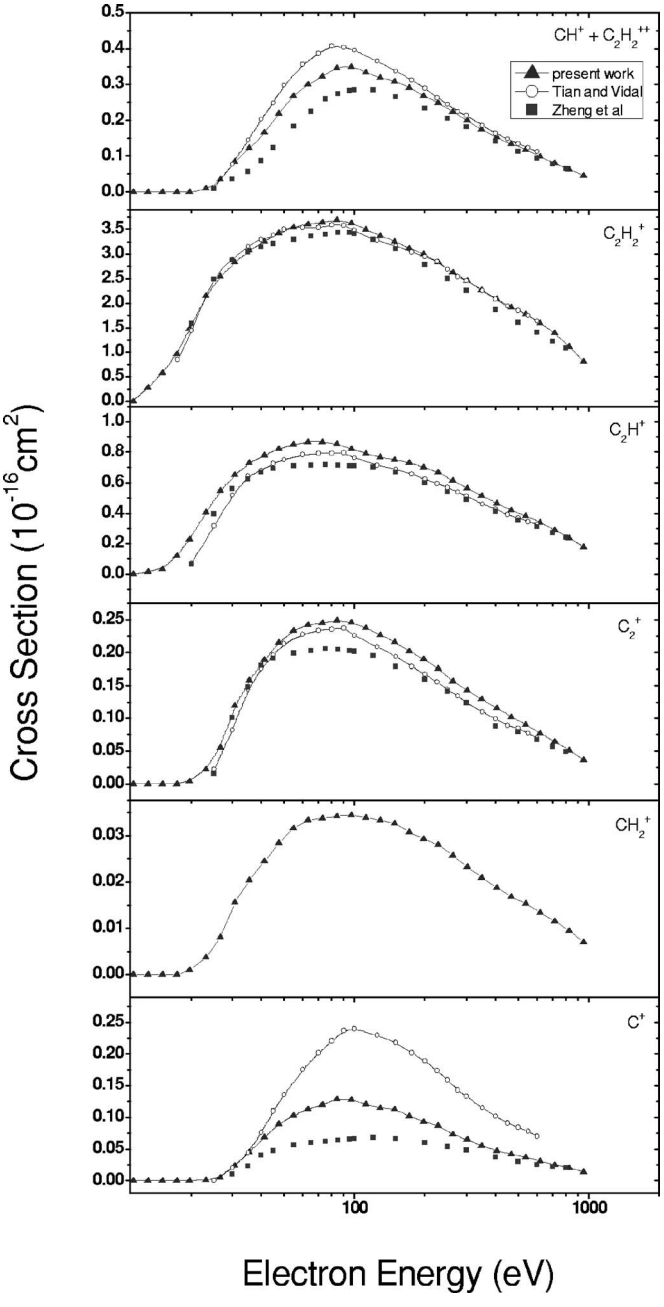

FIG. 5. Absolute partial cross sections for the ions $C_2H_2^+$, C_2H^+, C_2^+, C^+, CH_2^+, and CH^+ compared with cross sections obtained by Tian and Vidal (Ref. 11) and Zheng and Srlvastava (Ref. 8).

by Tian and Vidal.[11] Error bars for the partial cross sections before normalization with the data of Ref. 11 are estimated to lie within 15% (taking into account the error bars in the discrimination factors and in the measured ion currents). Within these error bars there is good agreement between the present partial cross section data and those of Tian and Vidal,[11] except for C^+ where the present cross sections are smaller by a factor of 2. It is interesting to note that the earlier data of Zheng *et al.*[8] (which did not take into account discrimination effects) are for all ions formed smaller than the present ones and those of Tian and Vidal.[11]

Cross section curves that are differential with respect to the kinetic energy of the ion (Fig. 6) can be deduced from the kinetic energy distributions and the partial cross sections (see

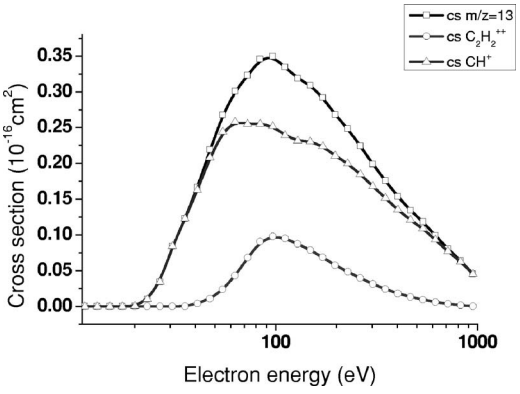

FIG. 6. Absolute partial cross section curve for ions at mass to charge ratio of 13 thomson (squares) and cross section curves for this mass per charge ratio that are differential with respect to the kinetic energy. Triangles mark the signal which is coming from ions with high kinetic energy (0.55–10 eV) and circles mark the ion yield coming from ions with rather low kinetic energies (0–0.5 eV). At around 40 eV we can see a strong increase in the slope of the low energy curve which marks the production of the doubly charged parent ion $C_2H_2^{++}$.

for details Ref. 23). The energy distribution function for the fragments CH_2^+ and CH^+ is divided into two parts: The range of the initial kinetic energy between 0 and 0.5 eV we call the thermal or low energy regime and initial kinetic energies higher than 0.5 eV are in the high energy regime. Figure 6 shows the absolute partial cross section curve of ions with the mass-to-charge ratio of 13 thomson (squares) and the separation of this curve into a low (0–0.5 eV, circles) and a high (0.5–10 eV, triangles) kinetic energy part. The curve of the ions with a low kinetic energy has a threshold of about 36 eV which corresponds nicely with the ionization energy of $^{13}C^{12}CH_2^{++}$ (Fig. 7). Ionization of C_2H_2 resulting in $C_2H_2^{++}$ does not change the momentum of the resulting ion and the z profiles of doubly charged parent ions are therefore narrow. Thus we can assign the low kinetic energy part of the cross section at a mass to charge ratio of 13 thomson to the formation of $^{12}C_2H_2^{++}$, whereas the high energy part is due to production of the fragment ions CH^+.

Figure 8 shows the separation of the cross section of CH_2^+ with $m/z=14$ thomson into a low and high kinetic energy contribution. We assign the curve with the higher appearance energy to a rearrangement reaction. Thissen *et al.*[27] argue that in the dicationic case the $C_2H_2^{++}$ is only slightly more stable than the isomeric form H_2CC^{++}. This suggests that the CH_2^+ can be formed as follows. First, the dicationic parent is formed which, after isomerization, decays into CH_2^+ and C^+. The appearance energy of the high kinetic energy curve corresponds approximately with the appearance energy of the doubly charged species. The low kinetic energy curve (E_{kin}=0–0.5 eV) can be attributed to the isotope $^{13}CH^+$. The appearance energy is the same as for $^{12}CH^+$ and the signal height is about 1% of the signal at a mass to charge ratio of 13 thomson.

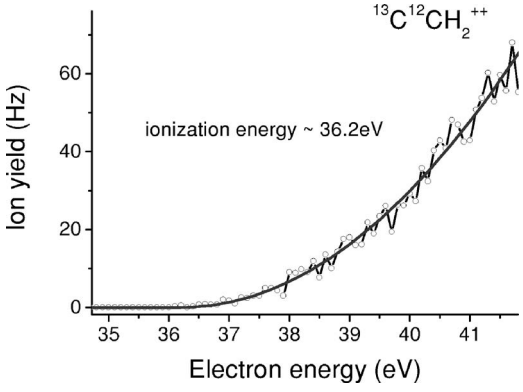

FIG. 7. Ion yield curve for the doubly charged parent ion measured on the isotope $^{13}C^{12}CH_2^{++}$ with mass per charge ratio of 13.5 thomson in order to avoid coincidences for $^{12}C_2H_2^{++}$ at mass of 13 thomson with the fragment CH^+ signal. Solid line is a Wannier-like fit through the data points allowing to deduce the appearance energy.

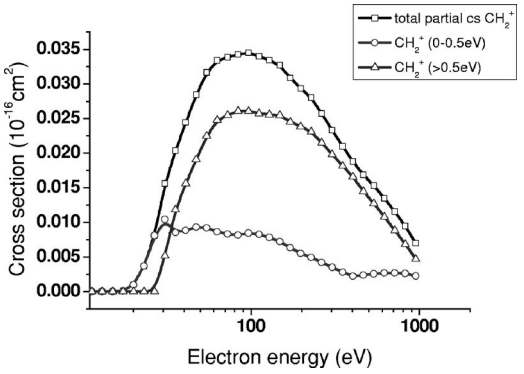

FIG. 8. Absolute partial cross section curve for the fragment ion CH_2^+ at mass per charge of 14 thomson (squares). The two kinetic energy regimes are shown separately by triangles and circles. One can see that the high energy curve (0.55–10 eV) starts at higher electron energies (~28 eV) and the low energy curve starts already at 18 eV.

Additional studies on the stability of the doubly charged parent ion have been performed. We observe a metastable decay reaction of the dicationic parent ion into $C_2H^+ + H^+$. The MIKE peak for this reaction is shown in Fig. 9. An analysis of this peak shape provides an average ⟨KER⟩ of 3.88 eV. Momentum conservation implies a kinetic energy for the heavier fragment ion C_2H^+ of about 0.2 eV. Our ⟨KER⟩ for this deprotonation reaction is in good agreement with the results of Thissen *et al.*[27] who performed a comprehensive analysis of the decay reactions of the ethyne dication. In addition to the deprotonation reaction $C_2H_2^{++} \rightarrow C_2H^+ + H^+$, they also observed the symmetric decay of the dication into $CH^+ + CH^+$ and the rearrangement reaction into $CH_2^+ + C^+$, mentioned above.

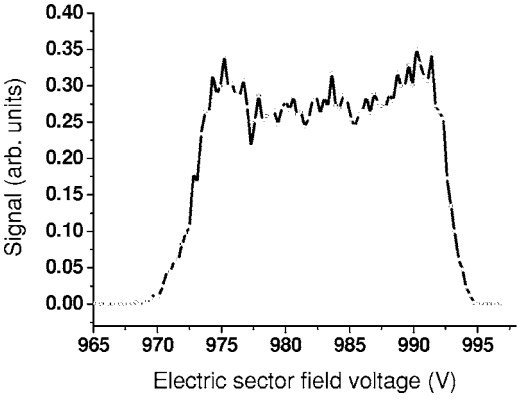

FIG. 9. MIKE—peak for the decay reaction $C_2H_2^{++} \rightarrow C_2H^+ + H^+$.

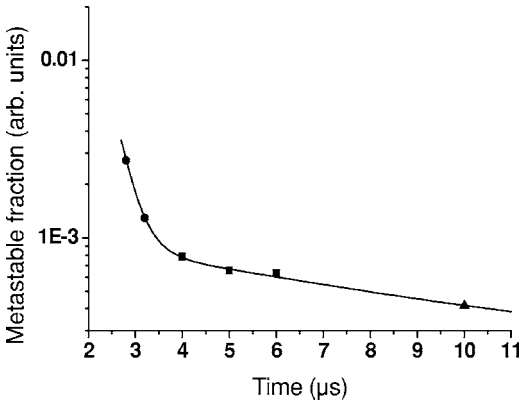

FIG. 10. Metastable fraction of the decay reaction $C_2H_2^{++} \rightarrow C_2H^+ + H^+$ as a function of time after the production of this ion in the ion source.

According to calculations of Thissen *et al.*, the deprotonation reaction occurs with a large energy release from the $^3\Pi_u$ excited state that has an accessible Franck-Condon region at about 37 eV above the neutral molecule. This state correlates directly with the ground state products along an entirely repulsive potential energy surface.

Moreover, besides this MIKE measurement, we also have determined the metastable fraction $[C_2H^+]/[C_2H^+] + [C_2H_2^{++}]$ as a function of the time after formation of the parent ion $C_2H_2^{++}$ in the ion source (see Fig. 10). These measurements have been performed with a recently constructed three sector field instrument[28] which enables us to investigate metastable decay reactions in three different field-free regions corresponding to three different time windows. By additionally changing the acceleration voltage from 3 down to 2 kV the time range can even be expanded (the circles correspond to the measurements in the first field-free region, the squares represent the metastable fraction measured in the second field-free region, and the triangle corresponds to the 3 kV measurement in the third field-free region). In a semilogarithmic plot such as Fig. 10 a linear dependence corresponds to a single lifetime. It turns out that the present data are not following a single-exponential curve but correspond to a double-exponential curve. By fitting the curve with a second order exponential fit (solid line) we obtain two lifetimes as fitting parameters. We deduce a lifetime of 0.3 μs for a fast decay channel and 7.3 μs for a second process that we attribute to the unimolecular deprotonation reaction of doubly charged acetylene as studied in Fig. 9.

ACKNOWLEDGMENTS

This work was partly supported by the FWF, Wien, and the European Commission, Brussels (network program), and has been performed within the Association EURATOM-ÖAW. The content of this publication is the sole responsibility of its publishers and it does not necessarily represent the views of the EU Commission or its services. One of the authors (T.D.M.) is an adjunct professor at Department of Experimental Physics, University, SK-84248 Bratislava, Slovak Republic.

[1] M. C. McMaster, W. L. Hsu, M. E. Coltrin, D. S. Dandy, and C. Fox, Diamond Relat. Mater. **4**, 1000 (1995).
[2] *Atomic and Molecular Processes in Fusion Edge Plasmas*, edited by R. K. Janev (Plenum, New York, 1995).
[3] H. W. Moos and J. T. Clark, Astrophys. J. **229**, L107 (1979).
[4] T. C. Owen, J. Caldwel, A. R. Rivolo, V. Moore, A. L. Lane, C. Sagan, H. Hunt, and C. Ponnamperuma, Astrophys. J. **236**, L39 (1987).
[5] J. T. Tate and P. T. Smith, Phys. Rev. **39**, 270 (1932).
[6] J. T. Tate, P. T. Smith, and A. L. Vaughan, Phys. Rev. **48**, 525 (1935).
[7] A. Gaudin and R. Hagemann, J. Chem. Phys. **64**, 1209 (1967).
[8] S. H. Zheng and S. K. Srivastava, J. Phys. B **29**, 3235 (1996).
[9] T. D. Märk and G. H. Dunn, *Electron Impact Ionization* (Springer Verlag, Berlin, 1985).
[10] T. Shirai, T. Tabata, H. Tawara, and Y. Itikawa, At. Data Nucl. Data Tables **80**, 147 (2002).
[11] C. Tian and C. R. Vidal, J. Phys. B **31**, 895 (1998).
[12] M. Davister and R. Locht, Chem. Phys. **189**, 805 (1994).
[13] M. Davister and R. Locht, Chem. Phys. **191**, 333 (1995).
[14] M. Davister and R. Locht, Chem. Phys. **195**, 443 (1995).
[15] P. Plessis and P. Marmet, Int. J. Mass Spectrom. Ion Process. **70**, 23 (1986).
[16] I. H. Suzuki and K. Maeda, Mass Spectrosc. (Tokyo) **25**, 223 (1977).
[17] P. Kusch, A. Hustrulid, and J. T. Tate, Phys. Rev. **52**, 843 (1937).
[18] M. A. Haney and J. L. Franklin, J. Chem. Phys. **48**, 4093 (1968).
[19] A. Bloch, Adv. Mass Spectrom. **2**, 48 (1968).
[20] H. U. Poll, V. Grill, S. Matt, N. Abramzon, K. Becker, P. Scheier, and T. D. Märk, Int. J. Mass Spectrom. Ion Process. **177**, 143 (1998).
[21] T. Fiegele, C. Mair, P. Scheier, K. Becker, and T. D. Märk, Int. J. Mass Spectrom. Ion Process. **207**, 145 (2001).
[22] V. Grill, G. Walder, P. Scheier, M. Kurdel, and T. D. Märk, Int. J. Mass Spectrom. Ion Process. **129**, 31 (1993).
[23] K. Gluch, P. Scheier, W. Schustereder, T. Tepnual, L. Feketeova, C. Mair, S. Matt-Leubner, A. Stamatovic, and T. D. Märk, Int. J. Mass Spectrom. Ion Process. **228**, 307 (2003).
[24] S. Feil, A. Bacher, M. Zangerl, W. Schustereder, K. Gluch, and P. Scheier, Int. J. Mass Spectrom. Ion Process. **233**, 325 (2004).
[25] J. H. Beynon, *Mass Spectrometry* (Elsevier, New York, 1960).
[26] K. Gluch, J. Fedor, S. Matt-Leubner, O. Echt, A. Stamatovic, M. Probst, P. Scheier, and T. D. Märk, J. Chem. Phys. **118**, 3090 (2003).
[27] R. Thissen, J. Delwiche, J. M. Robbe, D. Duflot, J. P. Flament, and J. H. D. Eland, J. Chem. Phys. **99**, 6590 (1993).
[28] S. Matt-Leubner, A. Stamatovic, R. Parajuli, P. Scheier, T. D. Märk, O. Echt, and C. Lifshitz, Int. J. Mass Spectrom. Ion Process. **222**, 213 (2003).